Experimental and Molecular Pathology 97 (2014) 433–439

Contents lists available at ScienceDirect

Experimental and Molecular Pathology

journal homepage: www.elsevier.com/locate/yexmp

Analysis of biological and technical variability in gene expression assays from formalin-fixed paraffin-embedded classical Hodgkin lymphomas

Gabriela Vera-Lozada [a], Vanesa Scholl [a], Mário Henrique M. Barros [b], Davide Sisti [c], Michele Guescini [c], Vilberto Stocchi [c], Claudio Gustavo Stefanoff [d], Rocio Hassan [a,*]

[a] Bone Marrow Transplantation Center, Instituto Nacional de Câncer (INCA), Rio de Janeiro, Brazil
[b] Institute for Pathology, Unfallkrankenhaus Berlin, Berlin, Germany
[c] Department of Biomolecular Sciences, University of Urbino Carlo Bo Via I Maggetti, Urbino, Italy
[d] Coordination of Clinical Research, Instituto Nacional de Câncer (INCA), Rio de Janeiro, Brazil

ARTICLE INFO

Article history:
Received 5 September 2014
Accepted 12 September 2014
Available online 16 September 2014

Keywords:
RT-qPCR
FFPE-RNA
ANOVA-nested design
Experimental variability
Inhibitors
Cy_0 method

ABSTRACT

Formalin-fixed paraffin-embedded (FFPE) tissues are invaluable sources of biological material for research and diagnostic purposes. In this study, we aimed to identify biological and technical variability in RT-qPCR TaqMan® assays performed with FFPE-RNA from lymph nodes of classical Hodgkin lymphoma samples. An ANOVA-nested 6-level design was employed to evaluate *BCL2*, *CASP3*, *IRF4*, *LYZ* and *STAT1* gene expression. The most variable genes were *CASP3* (low expression) and *LYZ* (high expression). Total variability decreased after normalization for all genes, except by *LYZ*. Genes with moderate and low expression were identified and suffered more the effects of the technical manipulation than high-expression genes. Pre-amplification was shown to introduce significant technical variability, which was partially alleviated by lowering to a half the amount of input RNA. *Ct* and Cy_0 quantification methods, based on cycle-threshold and the kinetic of amplification curves, respectively, were compared. Cy_0 method resulted in higher quantification values, leading to the decrease of total variability in *CASP3* and *LYZ* genes. The mean individual noise was 0.45 (0.31 to 0.61 SD), indicating a variation of gene expression over ~1.5 folds from one case to another. We showed that total variability in RT-qPCR from FFPE-RNA is not higher than that reported for fresh complex tissues, and identified gene-, and expression level-sources of biological and technical variability, which can allow better strategies for designing RT-qPCR assays from highly degraded and inhibited samples.

1. Introduction

Formalin-fixed and paraffin-embedded (FFPE) tissues are invaluable sources of biological material for pathologic analysis and molecular diagnosis (Fairley et al., 2012). However, in this type of sample, recovery of RNA appropriate for molecular analysis is complicated by degradation and the cross-link between RNA and proteins after formaldehyde fixation (Masuda et al., 1999).

Reverse transcription quantitative real-time PCR (RT-qPCR) is the gold standard technique for gene expression analysis, however, in FFPE samples amplification is affected by both, degradation and the presence of co-extracted inhibitors, leading to amplification at high values of cycles of quantification (*Cq*) (Godfrey et al., 2000; Koch et al., 2006), hence associated with increased variability and loss of linearity.

Besides the technical restrictions imposed by the nature of the RNA-FFPE samples, there is an underscored aspect of gene expression studies, which is the complexity of the tissue investigated. This factor imposes the amount of biological variability to be surpassed in order to detect a meaningful biological difference (Kitchen et al., 2010). In this respect, classical Hodgkin lymphoma (cHL) is one of the most complex cancers known; where tumor cells account for only 0.5–2% of tumor mass and are surrounded by variable numbers and types of inflammatory cells (Steidl et al., 2011). Gene expression profiles (GEP) corresponding to both, tumor and microenvironment compartments have been identified in this disease and have shown to carry useful prognostic information (Chetaille et al., 2009; Sánchez-Aguilera et al., 2006). This has lead to an ongoing interest in the development of sets of qPCR assays based on FFPE-RNA (Sanchez-Espiridion et al., 2010; Scott et al., 2013;

Abbreviations: *BCL2*, B-cell CLL/lymphoma2; *CASP3*, caspase 3; cHL, classical Hodgkin lymphoma; *Cq*, cycles of quantification; *Ct*, cycle threshold; CV, coefficient of variation; FFPE, formalin-fixed and paraffin-embedded; GOI, genes of interest; *GUSB*, glucuronidase beta; *HMBS*, hydroxymethylbilane synthase; *IRF4*, interferon regulatory factor 4; LN, lymph node; *LYZ*, lysozyme (renal amyloidosis); MIQE, Minimum Information for Publication of Quantitative Real-time PCR Experiments; Pre-Amp, pre-amplification; qPCR, quantitative real time PCR; REFG, reference gene; RIN, RNA integrity number; RT, reverse transcription; RT-qPCR, reverse transcription quantitative real-time PCR; SD, standard deviation; *STAT1*, signal transducer and activator of transcription 1.

* Corresponding author at: Oncovirology Laboratory, Bone Marrow Transplantation Center (CEMO), Instituto Nacional de Câncer — INCA, Praça Cruz Vermelha 23, 6° Andar, 20230-130, Rio de Janeiro, RJ, Brazil.
E-mail address: chassan@inca.gov.br (R. Hassan).

http://dx.doi.org/10.1016/j.yexmp.2014.09.014
0014-4800/

Venkataraman et al., 2014) to be used for clinical prediction in cHL, but no study has yet evaluated the sources of variability in RT-qPCR assays from FFPE-RNA.

Different approaches have been proposed for evaluating the variability in RT-qPCR assays (Bengtsson et al., 2008; Tichopad et al., 2009; Weaver et al., 2010). Among them, the nested-ANOVA design is a hierarchical approach suited to quantify the biological differences among subjects and the technical noise introduced by sample processing; each subject receives one treatment condition, and errors are linearly accumulative in each level (Fisher, 1935; Quinn and Keough, 2002).

In this work, we applied experimental designs as well as quantification approaches to evaluate specific RT-qPCR assays from FFPE-samples from cHL lymph nodes, in order to obtain useful information for diagnostic and prognostic test development.

2. Material and methods

Minimum Information for Publication of Quantitative Real-time PCR Experiments (MIQE) is listed in Appendix A.

2.1. Ethics statement

This study has been approved by the Instituto Nacional de Câncer (INCA) Ethics Committee, and has been performed in accordance with the ethical standards of the Declaration of Helsinki. Samples from patients were used after signed informed consent.

2.2. Samples

FFPE lymph nodes (LN) from 25 cHL diagnosed at the INCA, Brazil were included in the initial phase of this study. For the ANOVA-nested PCR assay, three subjects with cHL of the nodular sclerosis histological subtype were selected from the initial group by an experienced pathologist (MHMB), based on extensive immunohistochemistry characterization (Barros et al., 2010; Barros et al., 2012), and availability of two different FFPE-blocks from the same LN with similar tumor/stroma proportions.

2.3. Extraction of total RNA from FFPE lymph nodes

Total RNA was obtained from five microtomized sections using a Master Pure™ RNA purification Kit, Epicentre, following the supplier instructions except by the use of 480 μl tissue-and-cell-lysis solution with 60 μl of 60 mg/ml proteinase K (Invitrogen) and incubation at 65 °C for 20 h (Chen et al., 2007), followed by a treatment with 5 U/μl *DNaseI* at 37 °C for 30 min. RNA was resuspended in 12 μl of RNase-free water (Appendix A).

2.4. Reverse transcription

Reverse transcription (RT) was performed with the High-capacity cDNA Archive kit (Applied Biosystems, Life Technologies) from 1 μg of total RNA in 20 μl final volume (10 μl of diluted RNA and 10 μl RT mix). The reaction was incubated at 25 °C for 10 min and at 37 °C for 120 min in a Veriti™ Thermal Cycler (Applied Biosystems).

2.5. Pre-amplification step

Pre-amplification (Pre-Amp) was performed with the TaqMan® PreAmp Master Mix (Applied Biosystems) in a 10 μl-multiplex reaction which included primers and probes for all assays. According to the supplier, multiplex assays were designed to include up to 100 primers/probe sets, without introducing significant variability (Applied, 2010). Pre-Amp products were diluted 1:20 in RNase/DNase-free water and used for qPCR analysis.

2.6. qPCR assays

PCR quantifications were performed in an ABI7000 (Applied Biosystems) using TaqMan® chemistry, in duplicate, using cycle threshold (*Ct*) with fixed thresholds. The mean qPCR accepted standard deviation (SD) was 0.15 cycles. Additionally, kinetic parameters of the curve were used to calculated the Cy_0 as described (Guescini et al., 2008), based on Richards' equation with five parameters. This method does not require the assumption of similar efficiency in amplification of the genes of interest (GOI) and reference genes.

GOI were selected based on previous descriptions of clinically relevant genes in cHL (Sánchez-Espiridión et al., 2009) (Appendix A), and *GUSB* and *HMBS* were used as reference genes (REFG). RT-qPCR assay efficiencies ranged from 94.9 to 100.8% (Appendix B, Fig. B.1). All values of relative expression were expressed as $2^{-\Delta Cq}$.

2.7. Performance of RNA extractions

RNA quantity and quality were evaluated by spectrophotometry (Nanodrop®, ND-1000 Spectrophotometer) at OD 260 and OD 260/280/230 ratios; and by microfluidics technology for RNA integrity number (RIN) algorithm (2100 Bioanalyzer, Agilent Technologies). *Ct*-values < 35 cycles of both REFG amplifications defined an "amplifiable" sample.

2.8. Nested assay

A nested 6-level design ($3 \times 2 \times 2 \times 2 \times 2 \times 2$) was used to investigate the source of variability (biological and technical), in which two different FFPE blocks from the same LN from 3 cHL cases were analyzed, with duplicated RNA extractions, followed by duplicated retrotranscriptions, Pre-Amp and qPCR steps (Fig. 1).

2.9. Statistical analyses

Mann–Whitney's test was used to analyze associations between dichotomous and continuous non-normal variables, Wilcoxon signed-rank test was used to test the relation between paired samples and Spearman's test was used for correlating continuous variables. The linear model of the biological and technical processing effects was calculated as described by Tichopad et al. (2009) as: $Cq_{ijklmn} = \mu + a_i + b_{j(i)} + c_{k(ji)} + d_{l(kji)} + e_{m(lkji)} + f_{n(mlkji)}$.

Analyses were performed by nested-ANOVA of 6 factors with random effects. Variance partition was calculated as: $100 \times \sigma^2_x/\sigma^2_{Cq'}$, being $x = i, j, k, l, m, n$; as described in Kitchen et al. (2010). Statistical analyses were carried out with GENEX enterprise (MultiD), SPC (BPI Consulting, LLC) and Statistical Package for the Social Sciences 20.0 (SPSS) software. Figures were constructed with the GraphPad Prism 6 and Photoshop CC software.

3. Results

3.1. RNA extraction and GOI expression

From the 25 selected cHL LN, RNA mean yield was 696.3 ng/μl ± 578.4 SD. DNA purity was acceptable, with means 260/280 OD ratio of 1.81 ± 0.16, and 260/230 OD ratio of 1.75 ± 0.36. RIN values ranged from 2.2 to 4.8 (mean 2.46).

Pre-Amp procedure resulted in a significant gain of sensitivity, the inclusion of this step leading to an average increase of 10.1 ± 1.5 *Ct* in *GUSB* amplifications.

Expression levels of GOI are shown in Table 1 and Fig. 2. Means varied from $2^{-\Delta Ct}$ 4.300 to −3.911, allowing genes to be classified in highly expressed (*LYZ*, *STAT1* and *IRF4*), moderately expressed (*BCL2*), and low expressed genes (*CASP3*).

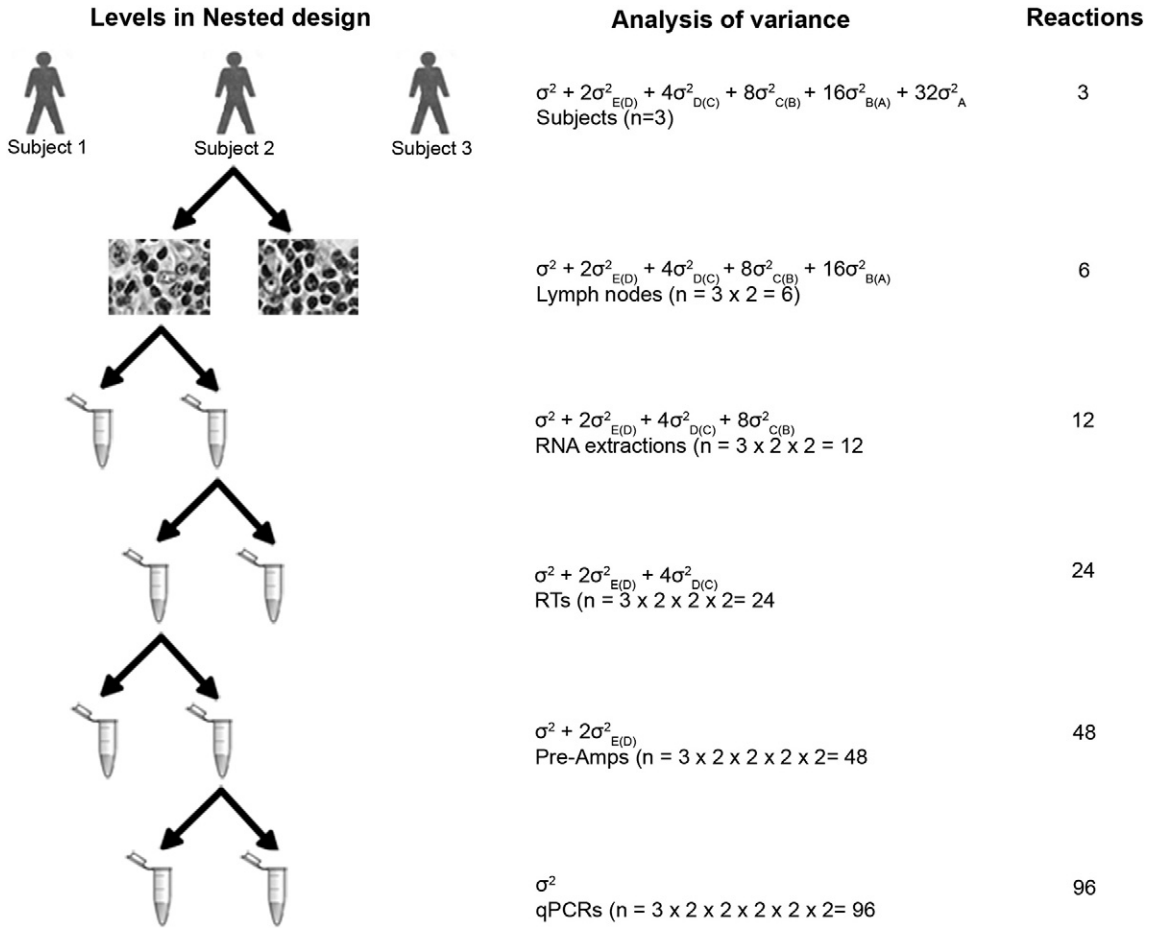

Fig. 1. Nested-ANOVA design of experiment.

3.2. Identification of sources of variability by a nested-ANOVA assay

The first experiment aimed to evaluate the performance of REFG, showing that *GUSB* performed better than *HMBS* (*Ct* means 23.085 SD ± 0.120 vs. 24.017 SD ± 0.139 for *HMBS*). Subjects #1 and #2 consistently crossed threshold at 2 *Ct*-values before subject #3 in REFG and the 5 analyzed GOI (Appendix B, Fig. B.2). This variability might have been caused by the presence of inhibitors in subject #3, or by unrecognized technical issues. Since the observed inter-subject variability may reflect the actual conditions when working with biological samples we decided to analyze the three subjects together.

GUSB Ct values were evaluated in 5 independent plates, and the assays were considered reproducible, with inter-assay variation of 2.07% CV for subject #1, 1.71% CV for subject #2, and 2.03% CV for subject #3 (mean CV 1.94%).

Table 1
Relative expression levels and variability of genes of interest (GOI) in a group of 25 Hodgkin lymphoma samples.

GOI	Median $2^{-\Delta Ct}$	Mean $2^{-\Delta Ct}$	SD	95% CI
LYZ	4.300	4.328	±1.270	4.020–4.637
STAT1	3.181	3.267	±0.902	3.004–3.530
IRF4	1.100	1.243	±1.240	0.989–1.497
BCL2	−1.860	−1.922	±1.547	−(2.230–1.615)
CASP3	−3.911	−3.889	±2.066	−(4.182–3.595)

SD: standard deviation; CI: confidence interval.

GOI mean expression recorded in the nested-ANOVA assays fell into the 95% coefficient interval of the whole group means (Table 1), and total variability values, calculated as the sum of biological and technical variability in the nested-assay, agreed with the SD of the whole group, for each of the analyzed GOI, as can be concluded by a comparison of means and total SDs in Tables 1 and 2.

3.3. Partition of variability (Ct-values)

The biological variability was >80% for all genes (Fig. 3A; Table C.1). Significant technical variability arose in the LN (*LYZ*); RNA (1.3% *LYZ* to 7.1% *CASP3*) and Pre-Amp stages (0.6% *IRF4* to 6.0% *CASP3*) (Fig. 3A; Appendix C, Table C.1). Analysis of the cumulative SD of *Ct*-values showed that *LYZ* was the gene with the highest total variability, while *IRF4* and *STAT1* exhibited the lowest total variability (Fig. 3B; Appendix C, Table C.2).

3.4. Effect of normalization on variability

Normalization allows referring expression levels to the amount of nucleic acid input (Bustin et al., 2009; Pfaffl, 2006; Vandesompele et al., 2002) but not necessarily leading to a decrease of variability (Kitchen et al., 2010). In our assays, after normalization, the total variability decreased for all GOI (mean SD ± 0.65), except for *LYZ* (Table 2; Fig. 4A). Regarding biological variability, *LYZ* showed the highest (SD ± 0.832) and *STAT1*, the lowest variability (SD ± 0.090) (Table 2). Variability in the RNA step decreased, while the technical

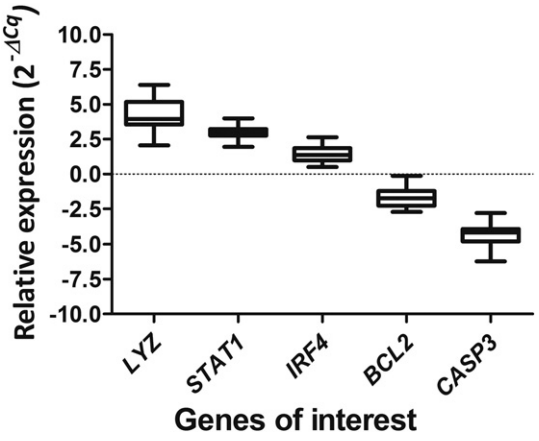

Fig. 2. Classification of genes by expression levels in 3 cases of classical Hodgkin lymphoma evaluated in the Nested design. In the box plot, the bar inside the box represents the median expression for each gene, the variation around the bar represents the values between 25 and 75 quartiles and the whiskers represent de minimum and maximum quantification value. Each value was expressed in $2^{-\Delta Ct}$ after normalization with a reference gene (*GUSB*).

variability introduced by the Pre-Amp step persisted significant for all genes.

3.5. Sources of variability according to gene expression level

Variability was analyzed in respect of expression levels, since previous work showed the effect of the gene expression level in the way that variability affects a given gene (Tichopad et al., 2009). Genes of moderate and lower expression suffered more the effects of the technical manipulation than genes of higher expression (average SD ± 0.930 vs. ±0.541, respectively). *STAT1* and *IRF4* were less affected by the technical variability, while *CASP3* exhibited a profound technical effect (Table 2).

3.6. Modifications of the pre-amplification step to reduce variability

A new set of five-level nested-ANOVA assays were designed (LN, RNA, RT, Pre-Amp and qPCR), aiming to evaluate the impact of assay modifications in variability. For this purpose, subject #2 (less variability and lower *Ct* values) was chosen, and *CASP3* (low expression and highest technical variability) and *STAT1* (high expression and lowest technical variability) were tested as GOI.

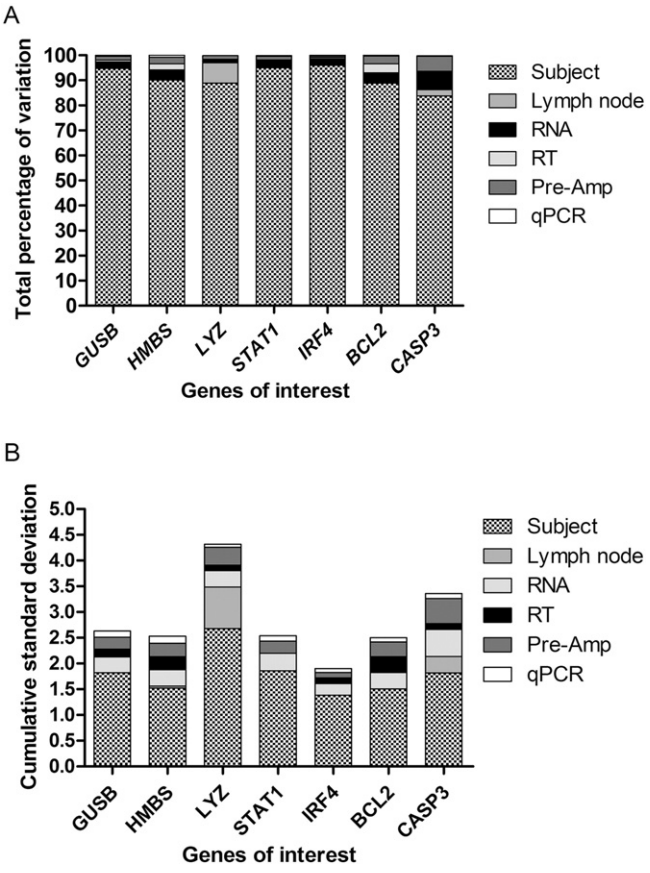

Fig. 3. Total variation attributed to each level of the nested-ANOVA assay in *Ct* values for reference genes and genes of interest. A: Percent partition; B: total standard deviation.

The initial Pre-Amp protocol (14 cycles and 1:20 final dilution) was changed to (i) 14 cycles, 1:10 dilution; and (ii) 10 cycles, 1:10 dilution, with no improvement in the technical variability introduced for each gene. Modification in the input RNA (1.0 to 0.5 μg, maintaining 14 cycles, 1:20 dilution), leads to a decrease of the biological and technical variability in *Ct*-values (*CASP3* and *STAT1*) and Δ*Ct*-values (*STAT1*)

Table 2
Nested-ANOVA assay-estimation of variability in subjects and sample processing steps in $2^{-\Delta Ct}$ and $2^{-\Delta Cy0}$ values.

	ΔCt genes of interest					ΔCy_0 genes of interest				
	LYZ	*STAT1*	*IRF4*	*BCL2*	*CASP3*	*LYZ*	*STAT1*	*IRF4*	*BCL2*	*CASP3*
Means	4.218	3.029	1.422	−1.679	−4.340	4.322	4.537	1.832	−2.004	−3.412
Biological variability										
Inter-subjects (SD)	0.832	0.090	0.491	0.548*	0.318	1.163**	0.314	0.516	0.567*	0.000
Technical variability										
Lymph nodes (SD)	0.601*	0.154	0.248*	0.000	0.170	0.000	0.229	0.224*	0.163*	0.346
RNA (SD)	0.208	0.000	0.066	0.120	0.280	0.000	0.104	0.042	0.000	0.207
RT (SD)	0.000	0.139	0.145	0.173	0.134	0.264	0.000	0.130	0.217	0.000
Pre-Amp (SD)	0.485**	0.346**	0.194**	0.362**	0.547**	0.430**	0.235**	0.201**	0.295**	0.666**
qPCR (SD)	0.106	0.103	0.090	0.124	0.120	0.136	0.177	0.184	0.352	0.112
Total technical variability (sum SD)	1.400	0.742	0.743	0.779	1.251	0.830	0.745	0.781	1.027	1.331
Total variability (sum SD biological and technical)	2.232	0.832	1.234	1.327	1.569	1.993	1.059	1.297	1.594	1.331
Total noise (SD)	1.024	0.388	0.533	0.624	0.702	1.070	0.454	0.560	0.669	0.712
Individual noise (SD)	0.601	0.346	0.306	0.405	0.610	0.448	0.342	0.334	0.460	0.651

* *P*-value < 0.05; ** *P*-value < 0.01.

Ct: threshold cycle; Cy_0: Cy_0 quantification; SD: standard deviation. RT: retrotranscription; Pre-Amp: pre-amplification; qPCR: quantitative real-time PCR. Total noise was calculated as the accumulative variation expressed in SD values of all quantifications in $2^{-\Delta Cq}$ values for the 3 subjects as if they had been obtained independently. Individual noise was calculated as $\sum$ SD for each Δ*Cq* by subjects/number of subjects, being *Cq* values expressed either as *Ct* or Cy_0. *P*-values obtained from nested ANOVA analyses.

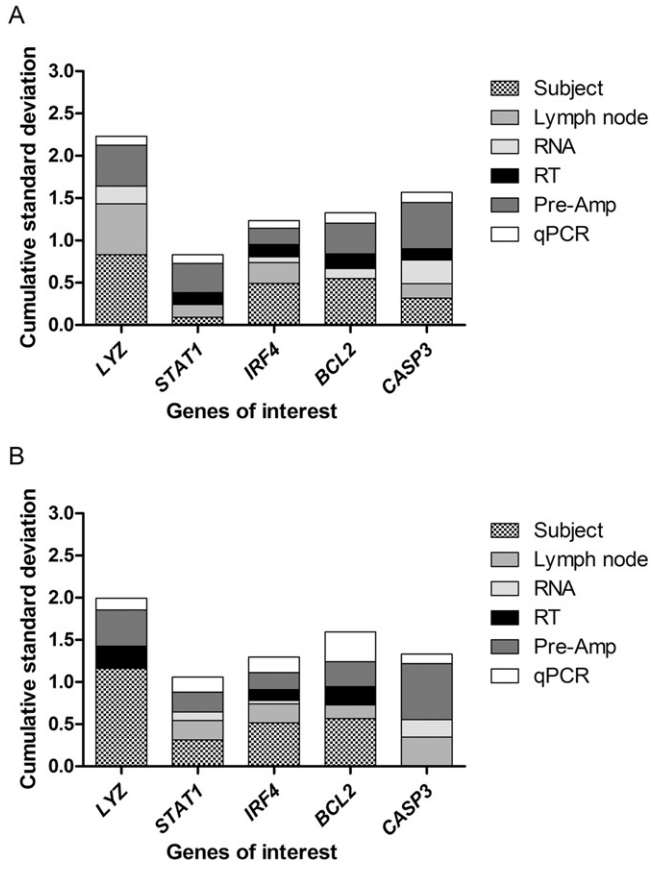

Fig. 4. Distribution of the cumulative standard deviation by biological and technical steps after normalization. A: ΔCt values. B: $\Delta Cy0$ values.

(Appendix B, Fig. B.3). Reducing to half (2.5 to 1.25 μl) the amount of cDNA in Pre-Amp reactions did not lead to additional variability decrease.

3.7. Evaluation of quantification methods: Cy_0 vs. Ct

The nested-ANOVA results were re-evaluated with Cy_0-values, aiming to identify a putative effect of inhibitors in PCR reactions. Significantly higher expression values in Cy_0 quantifications were observed (96 qPCR) for all genes ($P < 0.001$, Wilcoxon test), except for *LYZ* ($P = 0.120$).

In general, variability in each of the ANOVA-levels was similar regardless of the quantification method (*Ct* or Cy_0). However, with the last method, the total biological variability decreased for *LYZ* and *CASP3*, whereas technical variability was not affected. The Pre-Amp variability was unaffected by the quantification method or gene analyzed, indicating that the error introduced in this stage is specific of this technical step and not gene- or inhibitor-dependent (Table 2 and Fig. 4B).

4. Discussion

Nowadays, much emphasis is being placed on the collection of precise information about pre-analytical and analytical qPCR conditions to contribute to science repeatability and technical reproducibility, which is led by initiatives such as the MIQE proposal (Bustin et al., 2009). In the gene-expression biomarker validation setting, where qPCR methodologies have a consolidated place, reproducibility is indeed a great concern; however, migrating from discovery technologies to routine RT-qPCR assays has not yet reached the optimal validation and analysis tools observed in other areas of molecular diagnosis (Murphy and Bustin, 2009).

Tichopad et al. (2009) were the first to apply a nested ANOVA design to investigate the extent of the variability included in each experimental stage, and showed that the biological variability increases along with the complexity of tissues, being higher in the solid tissues than in peripheral blood and cell lines. They also described a not-yet-understood gene-specific component that affects variability. This approach has not been applied for the evaluation of FFPE-RNA; thus, we sought to expand the design for its application in this troublesome type of samples.

In our study, the total noise observed for the REFG (SD mean, 23.55 + 1.45 cycles) was similar to those reported for *ACTB* expression in fresh solid tissue (liver) (Kitchen et al., 2010). The GOI mean total noise (1.57 cycles ± 1.17–1.68, excluding *LYZ*) was also similar to that published for fresh tissues (mean 1.3; SD ± 1.0–1.7), indicating that using RNA-FFPE does not lead to a significant increase of variability in RT-qPCR assays.

The technical variability was higher in our study than in the reference work (Tichopad et al., 2009) (SD mean ± 0.86 vs. ±0.67), which is justified by our 5-level design vs. only two (RT and qPCR) (Tichopad et al., 2009). Nevertheless, the genes with the highest technical variability in both studies exhibited comparable SD values (*CASP3* vs. *FGF7*, ±1.23 and ±1.29, respectively).

In respect to sources of technical variability, pre-amplification is a strategy that has increasingly been used to improve the amplification of mRNA from FFPE tissues, and to increase the sensitivity of qPCR for low expression genes (Denning et al., 2007; Li et al., 2008; Noutsias et al., 2008). In line with this, we showed that a significant number of samples considered not amplifiable ($Ct \geq 35$), were recovered by the Pre-Amp technical application. However, this was obtained at the expense of introducing significant technical variability in all genes. Decreasing the amount of input RNA partially alleviated the effect of Pre-Amp on the variability, suggesting the inhibitors present in FFPE-RNA affected the efficiency of the retrotranscription step (Tichopad et al., 2004), effect that may have been dragged into the next, Pre-Amp level.

The presence of inhibitors is an unavoidable issue in FFPE-RNA samples, which effects are neither well captured by the ANOVA design since they do not propagate linearly from the superior to the inferior levels in the hierarchical model (Bar et al., 2012; Godfrey et al., 2000; Tichopad et al., 2004), nor, ultimately by the *Ct* quantification method. The last is due mainly because inhibitors in biological samples can alter the efficiency of qPCR reactions (Bar, 2003; Tichopad et al., 2004; Tichopad et al., 2010), violating the similar efficiency principle that has to be assumed for using the *Ct* method (Livak and Schmittgen, 2001; Pfaffl, 2001). Different approaches have been described for studying qPCR kinetics to avoid the utilization of external curves (Bar et al., 2012; Ruijter et al., 2013), among them, the Cy_0 quantification method has been previously used to disclose the effects of inhibition on the kinetic of the amplification curve applying a mathematical algorithm based on Richard's equation (Guescini et al., 2008). Then, we decided to compare the performance of *Ct* and Cy_0 quantification methods in decreasing variability of TaqMan®-based RT-qPCR assays from FFPE-samples.

The use of Cy_0-quantified values in the ANOVA-nested design allowed to observe a decrease in total variability in genes such as *LYZ* and *CASP3* (highest total and technical variability, respectively). Importantly, the decrease in variability was evident in the upper (biological) levels, which can be interpreted as the effect of inhibitor dilution from the upper to the lower steps (Bar et al., 2012; Tichopad et al., 2009). These data clearly demonstrated, for the first time, that Cy_0 algorithm can effectively account for slight curve shifting due to small variations in PCR efficiency present in very complex biological tissues as FFPE-samples.

In the field of cHL clinical research, there is an ongoing interest in the development of sets of qPCR assays based on FFPE-RNA (Sanchez-Espiridion et al., 2010; Scott et al., 2013; Venkataraman et al., 2014), to be used for clinical prediction, a goal that has been accomplished with certain success in other neoplasms such as breast cancer (van de Vijver et al., 2002; Wang et al., 2005). In this respect, the

variability detected in this study, quantified for instance by the individual noise, ranged between 0.31 and 0.61 SD (mean 0.45) showing that expression levels would vary over ~1.5 folds from one case to another. This indicates a high threshold for a given gene to achieve, which should be taken into account when defining any cutoff value to allocate patients in molecular risk groups for clinical purposes.

The results of this study raise attention to several practical issues. In respect to the statistical power of the experimental design, our results point to an increase in biological replicates, and no impact of evaluating more than one lymph node, or RNA aliquots/RT-reactions. We also identified a precise requirement to optimize the Pre-Amp step as the more sensitive technical source of variability, and draw attention to the need of using Pre-AMP step in all samples, and not only in the ones that amplify at high *Cq* levels of REFG, in order to homogenization of introduced errors.

In sum, we showed that the use of RNA-FFPE does not lead to an increase in variability in RT-qPCR assays than that reported for fresh tissues; and identified gene-, and expression level-sources of biological and technical variability, which can allow better strategies for RT-qPCR designs from highly degraded and inhibited samples.

Supplementary data to this article can be found online at http://dx.doi.org/10.1016/j.yexmp.2014.09.014.

Conflict of interest statement

The authors declare that there are no conflicts of interest.

Role of the funding source

The funders had no role in study design, data collection and analysis, decision to publish, or preparation of the manuscript.

Acknowledgments

This work was supported by grants from INCT para controle do câncer (grants CNPq 573806/2008-0 and FAPERJ E-26/110.432/2010) (Brazil) and the Fundação de Amparo à Pesquisa do Rio de Janeiro (FAPERJ) projects E-26/111.429/2012 (RELINFO) and E-26/110.238/2014 (PP-SUS program) (Brazil). MHMB was supported by a fellowship from the Alexander von Humboldt Foundation (Germany). GVL and RH would like to thank Drs I. Zalcberg and P. Cappelletti for their support during the first stage of this work.

References

Applied, B., 2010. TaqMan® PreAmp Master Mix Kit Protocol.

Bar, T., 2003. Kinetic outlier detection (KOD) in real-time PCR. Nucleic Acids Res. 31, e-105. http://dx.doi.org/10.1093/nar/gng106.

Bar, T., Kubista, M., Tichopad, A., 2012. Validation of kinetics similarity in qPCR. Nucleic Acids Res. 40, 1395–1406. http://dx.doi.org/10.1093/nar/gkr778.

Barros, M.H.M., Scheliga, A., De Matteo, E., Minnicelli, C., Soares, F.A., Zalcberg, I.R., Hassan, R., 2010. Cell cycle characteristics and Epstein–Barr virus are differentially associated with aggressive and non-aggressive subsets of Hodgkin lymphoma in pediatric patients. Leuk. Lymphoma 51, 1513–1522. http://dx.doi.org/10.3109/10428194.2010.489243.

Barros, M.H.M., Vera-Lozada, G., Soares, F.A., Niedobitek, G., Hassan, R., 2012. Tumor microenvironment composition in pediatric classical Hodgkin lymphoma is modulated by age and Epstein–Barr virus infection. Int. J. Cancer 131, 1142–1152. http://dx.doi.org/10.1002/ijc.27314.

Bengtsson, M., Hemberg, M., Rorsman, P., Ståhlberg, A., 2008. Quantification of mRNA in single cells and modelling of RT-qPCR induced noise. BMC Mol. Biol. 9, 63. http://dx.doi.org/10.1186/1471-2199-9-63.

Bustin, S.A., Benes, V., Garson, J.A., Hellemans, J., Huggett, J., Kubista, M., Mueller, R., Nolan, T., Pfaffl, M.W., Shipley, G.L., Vandesompele, J., Wittwer, C.T., 2009. The MIQE guidelines: minimum information for publication of quantitative real-time PCR experiments. Clin. Chem. 55, 611–622. http://dx.doi.org/10.1373/clinchem.2008.112797.

Chen, J., Byrne Jr., G.E., Lossos, I.S., 2007. Optimization of RNA extraction from formalin-fixed, paraffin-embedded lymphoid tissues. Diagn. Mol. Pathol. 16, 61–72.

Chetaille, B., Bertucci, F., Finetti, P., Esterni, B., Stamatoullas, A., Picquenot, J.M., Copin, M.C., Morschhauser, F., Casasnovas, O., Petrella, T., Molina, T., Vekhoff, A., Feugier, P., Bouabdallah, R., Birnbaum, D., Olive, D., Xerri, L., 2009. Molecular profiling of classical Hodgkin lymphoma tissues uncovers variations in the tumor microenvironment and correlations with EBV infection and outcome. Blood 113, 2765–3775. http://dx.doi.org/10.1182/blood-2008-07-168096.

Denning, K.M., Smyth, P.C., Cahill, S.F., Finn, S.P., Conlon, E., Li, J., Flavin, R.J., Aherne, S.T., Guenther, S.M., Ferlinz, A., 2007. A molecular expression signature distinguishing follicular lesions in thyroid carcinoma using preamplification RT-PCR in archival samples. Mod. Pathol. 20, 1095–1102.

Fairley, J.A., Gilmour, K., Walsh, K., 2012. Making the most of pathological specimens: molecular diagnosis in formalin-fixed, paraffin embedded tissue. Curr. Drug Targets 13, 1475–1487.

Fisher, R.A., 1935. The Design of Experiments. Oliver & Boyd, Oxford, England.

Godfrey, T.E., Kim, S.-H., Chavira, M., Ruff, D.W., Warren, R.S., Gray, J.W., Jensen, R.H., 2000. Quantitative mRNA expression analysis from formalin-fixed, paraffin-embedded tissues using 5′ nuclease quantitative reverse transcription-polymerase chain reaction. J. Mol. Diagn. 2, 84–91.

Guescini, M., Sisti, D., Rocchi, M.B.L., Stocchi, L., Stocchi, V., 2008. A new real-time PCR method to overcome significant quantitative inaccuracy due to slight amplification inhibition. BMC Bioinforma. 9, 326. http://dx.doi.org/10.1186/1471-2105-9-326.

Kitchen, R.R., Kubista, M., Tichopad, A., 2010. Statistical aspects of quantitative real-time PCR experiment design. Methods 50, 231–236. http://dx.doi.org/10.1016/j.ymeth.2010.01.025.

Koch, I., Slotta-Huspenina, J., Hollweck, R., Anastasov, N., Hofler, H., Quintanilla-Martinez, L., Fend, F., 2006. Real-time quantitative RT-PCR shows variable, assay-dependent sensitivity to formalin fixation: implications for direct comparison of transcript levels in paraffin-embedded tissues. Diagn. Mol. Pathol. 15, 149–156.

Li, J., Smyth, P., Cahill, S., Denning, K., Flavin, R., Aherne, S., Pirotta, M., Guenther, S.M., O'Leary, J.J., Sheils, O., 2008. Improved RNA quality and TaqMan® Pre-amplification method (PreAmp) to enhance expression analysis from formalin fixed paraffin embedded (FFPE) materials. BMC Biotechnol. 8, 10. http://dx.doi.org/10.1186/1472-6750-8-10.

Livak, K.J., Schmittgen, T.D., 2001. Analysis of relative gene expression data using real-time quantitative PCR and the $2^{-\Delta\Delta CT}$ method. Methods 25, 402–408. http://dx.doi.org/10.1006/meth.2001.1262.

Masuda, N., Ohnishi, T., Kawamoto, S., Monden, M., Okubo, K., 1999. Analysis of chemical modification of RNA from formalin-fixed samples and optimization of molecular biology applications for such samples. Nucleic Acids Res. 27, 4436–4443.

Murphy, J., Bustin, S.A., 2009. Reliability of real-time reverse-transcription PCR in clinical diagnostics: gold standard or substandard? Expert. Rev. Mol. Diagn. 9, 187–197. http://dx.doi.org/10.1586/14737159.9.2.187.

Noutsias, M., Rohde, M., Block, A., Klippert, K., Lettau, O., Blunert, K., Hummel, M., Kühl, U., Lehmkuhl, H., Hetzer, R., Rauch, U., Poller, W., Pauschinger, M., Schultheiss, H.P., Volk, H.D., Kotsch, K., 2008. Preamplification techniques for real-time RT-PCR analyses of endomyocardial biopsies. BMC Mol. Biol. 9, 3. http://dx.doi.org/10.1186/1471-2199-9-3.

Pfaffl, M.W., 2001. A new mathematical model for relative quantification in real-time RT-PCR. Nucleic Acids Res. 29, e45.

Pfaffl, M.W., 2006. Relative quantification. In: Dorak, M.T. (Ed.), Real-time PCR. Taylor & Francis Group, School of Clinical Medical Sciences (Child Health), Newcastle University, Newcastle-upon-Tyne, UK, pp. 63–82.

Quinn, G.P., Keough, M.J., 2002. Experimental Design and Data Analysis for Biologists. Cambridge University Press, Cambridge, UK; New York.

Ruijter, J.M., Pfaffl, M.W., Zhao, S., Spiess, A.N., Boggy, G., Blom, J., Rutledge, R.G., Sisti, D., Lievens, A., De Preter, K., Derveaux, S., Hellemans, J., Vandesompele, J., 2013. Evaluation of qPCR curve analysis methods for reliable biomarker discovery: bias, resolution, precision, and implications. Methods 59, 32–46. http://dx.doi.org/10.1016/j.ymeth.2012.08.011.

Sánchez-Aguilera, A., Montalbán, C., de la Cueva, P., Sánchez-Verde, L., Morente, M.M., García-Cosío, M., García-Laraña, J., Bellas, C., Provencio, M., Romagosa, V., de Sevilla, A.F., Menárguez, J., Sabín, P., Mestre, M.J., Méndez, M., Fresno, M.F., Nicolás, C., Piris, M.A., García, J.F., Spanish Hodgkin Lymphoma Study Group, 2006. Tumor microenvironment and mitotic checkpoint are key factors in the outcome of classic Hodgkin lymphoma. Blood 108, 662–668. http://dx.doi.org/10.1182/blood-2005-12-5125.

Sanchez-Espiridion, B., Montalban, C., Lopez, A., Menarguez, J., Sabin, P., Ruiz-Marcellan, C., Lopez, A., Ramos, R., Rodriguez, J., Canovas, A., Camarero, C., Canales, M., Alves, J., Arranz, R., Acevedo, A., Salar, A., Serrano, S., Bas, A., Moraleda, J.M., Sanchez-Godoy, P., Burgos, F., Rayon, C., Fresno, M.F., Larana, J.G., Garcia-Cosio, M., Santonja, C., Lopez, J.L., Llanos, M., Mollejo, M., Gonzalez-Carrero, J., Marin, A., Forteza, J., Garcia-Sanz, R., Tomas, J.F., Morente, M.M., Piris, M.A., Garcia, J.F., on behalf of the Spanish Hodgkin Lymphoma Study Group, 2010. A molecular risk score based on 4 functional pathways for advanced classical Hodgkin lymphoma. Blood 116, e12–e17. http://dx.doi.org/10.1182/blood-2010-02-270009.

Sánchez-Espiridión, B., Sánchez-Aguilera, A., Montalbán, C., Martin, C., Martinez, R., González-Carrero, J., Poderos, C., Bellas, C., Fresno, M.F., Morante, C., Mestre, M.J., Mendez, M., Mazorra, F., Conde, E., Castaño, A., Sánchez-Godoy, P., Tomas, J.F., Morente, M.M., Piris, M.A., García, J.F., Spanish Hodgkin's Lymphoma Study Group, 2009. xA TaqMan low-density array to predict outcome in advanced Hodgkin's lymphoma using paraffin-embedded samples. Clin. Cancer Res. 15, 1367–1375. http://dx.doi.org/10.1158/1078-0432.CCR-08-1119.

Scott, D.W., Chan, F.C., Hong, F., Rogic, S., Tan, K.L., Meissner, B., Ben-Neriah, S., Boyle, M., Kridel, R., Telenius, A., Woolcock, B.W., Farinha, P., Fisher, R.I., Rimsza, L.M., Bartlett, N.L., Cheson, B.D., Shepherd, L.E., Advani, R.H., Connors, J.M., Kahl, B.S., Gordon, L.I., Horning, S.J., Steidl, C., Gascoyne, R.D., 2013. Gene expression-based model using formalin-fixed paraffin-embedded biopsies predicts overall survival in advanced-stage classical Hodgkin lymphoma. J. Clin. Oncol. 31, 692–700. http://dx.doi.org/10.1200/JCO.2012.43.4589.

Steidl, C., Connors, J.M., Gascoyne, R.D., 2011. Molecular pathogenesis of Hodgkin's lymphoma: increasing evidence of the importance of the microenvironment. J. Clin.

Oncol. Off. J. Am. Soc. Clin. Oncol. 29, 1812–1826. http://dx.doi.org/10.1200/JCO.2010.32.8401.

Tichopad, A., Bar, T., Pecen, L., Kitchen, R.R., Kubista, M., Pfaffl, M.W., 2010. Quality control for quantitative PCR based on amplification compatibility test. Methods. 50, 308–312. http://dx.doi.org/10.1016/j.ymeth.2010.01.028.

Tichopad, A., Didier, A., Pfaffl, M.W., 2004. Inhibition of real-time RT-PCR quantification due to tissue-specific contaminants. Mol. Cell. Probes 18, 45–50. http://dx.doi.org/10.1016/j.mcp.2003.09.001.

Tichopad, A., Kitchen, R., Riedmaier, I., Becker, C., Stahlberg, A., Kubista, M., 2009. Design and optimization of reverse-transcription quantitative PCR experiments. Clin. Chem. 55, 1816–1823. http://dx.doi.org/10.1373/clinchem.2009.126201.

Van de Vijver, M.J., He, Y.D., van't Veer, L.J., Dai, H., Hart, A.A.M., Voskuil, D.W., Schreiber, G.J., Peterse, J.L., Roberts, C., Marton, M.J., Parrish, M., Atsma, D., Witteveen, A., Glas, A., Delahaye, L., van der Velde, T., Bartelink, H., Rodenhuis, S., Rutgers, E.T., Friend, S.H., Bernards, R., 2002. A gene-expression signature as a predictor of survival in breast cancer. N. Engl. J. Med. 347, 1999–2009. http://dx.doi.org/10.1056/NEJMoa021967.

Vandesompele, J., De Preter, K., Pattyn, F., Poppe, B., Van Roy, N., De Paepe, A., Speleman, F., 2002. Accurate normalization of real-time quantitative RT-PCR data by geometric averaging of multiple internal control genes. Genome Biol. 3 (research0034).

Venkataraman, G., Mirza, M.K., Eichenauer, D.A., Diehl, V., 2014. Current status of prognostication in classical Hodgkin lymphoma. Br. J. Haematol. 165, 287–299. http://dx.doi.org/10.1111/bjh.12759.

Wang, Y., Klijn, J.G.M., Zhang, Y., Sieuwerts, A.M., Look, M.P., Yang, F., Talantov, D., Timmermans, M., Meijer-van Gelder, M.E., Yu, J., Jatkoe, T., Berns, E.M.J.J., Atkins, D., Foekens, J.A., 2005. Gene-expression profiles to predict distant metastasis of lymph-node-negative primary breast cancer. Lancet 365, 671–679. http://dx.doi.org/10.1016/S0140-6736(05)17947-1.

Weaver, S., Dube, S., Mir, A., Qin, J., Sun, G., Ramakrishnan, R., Jones, R.C., Livak, K.J., 2010. Taking qPCR to a higher level: analysis of CNV reveals the power of high throughput qPCR to enhance quantitative resolution. Methods. 50, 271–276. http://dx.doi.org/10.1016/j.ymeth.2010.01.003.